

BRIEF COMMUNICATIONS

Design of Nonpeptidic Topomimetics of Antiangiogenic Proteins With Antitumor Activities

Ruud P. M. Dings, Xuemei Chen, Debby M. E. I. Hellebrekers, Loes I. van Eijk, Ying Zhang, Thomas R. Hoye, Arjan W. Griffioen, Kevin H. Mayo

The inhibition of angiogenesis is a promising avenue for cancer treatment. Although some angiostatic compounds are in the process of development and testing, these often prove ineffective in vivo or have unwanted side effects. We have designed, synthesized, and evaluated a small library of nonpeptidic, calixarene-based protein surface topomimetics that display chemical substituents to approximate the molecular dimensions and amphipathic features (hydrophobic and positively charged residues) of the antiangiogenic peptide anginex, which, like many antiangiogenic proteins, consists primarily of an antiparallel β -sheet structure as the functional unit. Two of the topomimetics (0118 and 1097) were potent angiogenesis inhibitors in vitro, as determined by endothelial cell proliferation, migration, and chick embryo chorioallantoic membrane assays. Moreover, both compounds were highly effective at inhibiting tumor angiogenesis and growth in two mouse models (MA148 human ovarian carcinoma and B16 murine melanoma). Our results demonstrate the feasibility of designing nonpeptidic protein surface topomimetics as novel pharmaceutical agents for clinical intervention against cancer through angiostatic or other mechanisms. [J Natl Cancer Inst 2006;98:932–6]

Angiogenesis is fundamental to both normal organ development and cancer progression (1), and agents that can

inhibit blood vessel development in tumors have shown promise as therapeutics (2,3). Although anti-vascular endothelial growth factor agents like bevacizumab (Avastin) are perhaps the most well known antiangiogenic compounds (4), many other antiangiogenic compounds have been identified and are currently being tested in clinical trials. The most promising are those that act directly on endothelial cells to inhibit tumor angiogenesis, thereby reducing the risk that drug resistance will develop and making the compounds more effective against a broad spectrum of tumors. However, angiogenesis inhibitors are often relatively ineffective in vivo or cause unwanted biologic side effects (5), underscoring the need for more and better angiostatic agents.

Most antiangiogenic proteins and peptides including endostatin, angiostatin, platelet factor 4, thrombospondin, gamma interferon-inducible protein 10, tumor necrosis factor, bactericidal/permeability increasing protein, thrombospondin type 1 repeat peptides, Flt-1 peptide (Fms-like tyrosine kinase 1 vascular endothelial growth factor receptor-derived peptide), and anginex share an antiparallel β -sheet structure and a preponderance of positively charged and hydrophobic residues (6). This compositional and structural similarity may prove useful in the design of additional antiangiogenesis agents. With the goal of developing novel and effective inhibitors of angiogenesis, we used the antiangiogenic peptide anginex as a model to design nonpeptidic compounds that approximate the molecular dimensions of the peptide, its hydrophobic and positively charged amino acid composition, and the surface topology of the functionally critical amphipathic β -sheet conformation (7) (Fig. 1, A). The structural unit encompassing key residues in anginex covers approximately the dimensions of a two-stranded β -sheet that is only about four amino acid residues in length on each strand (8). These overall backbone dimensions are similar to those of the calix[4]arene scaffold (Fig. 1, A). Adding hydrophobic and basic chemical groups to calix[4]arene can increase the molecular surface span on each side of the scaffold from about 8 Å to about 15 Å, approximating the maximum distance between side chains on one side of anginex. Calix[4]arenes can exist in four topological isomers (4-up, 3-up/1-down, and two 2-up/2-down)

that can, in principle, interconvert by rotation of the oxygenated “head” of each ring through the core (9). However, calix[4]arene derivatives bearing groups larger than ethoxy on the lower, more narrow rim (which includes all of those studied here) are essentially inert with respect to this topological change on the laboratory/pharmacology time scale. Moreover, even for derivatives unsubstituted *para* to the oxygenated carbon, rotation of the larger “tail” of the ring through the core is also too slow to be of consequence (10).

We synthesized 23 calix[4]arene analogs containing, in various combinations, chemical substituents from among those shown at right in Fig. 1, A. (Synthesis of the compounds used in this study is described in Supplemental Methods, available at <http://jncicancerspectrum.oxfordjournals.org/jnci/content/vol98/issue13>.) Most of these had four similar (i.e., hydrophobic or hydrophilic) groups on one rim (top or bottom) of the calix[4]arene cylinder. The specific structures of the three compounds discussed here are presented in Fig. 1, B.

For an initial assessment of the antiangiogenic potential of the compounds, we used a [³H]-thymidine incorporation assay, as described previously (11), that measures the proliferation of basic fibroblast growth factor (bFGF)-stimulated human umbilical vein-derived endothelial cells (HUVEC) in culture. Compounds 0118 and 1097 were found to be highly effective at inhibiting endothelial cell proliferation (Fig. 1, C), with 0118 (IC₅₀ [i.e., the concentration required for 50% inhibition of proliferation] = 2 μM, 95% confidence interval [CI] = 1.8 μM to 3.1 μM) being slightly more potent

Affiliations of authors: Departments of Biochemistry, Molecular Biology & Biophysics (RPM, KHM) and Chemistry (XC, TRH) and the Cancer Center (YZ, KHM), University of Minnesota, Minneapolis, MN; Angiogenesis Laboratory, Research Institute for Growth and Development, Department of Pathology, University Hospital Maastricht, The Netherlands (DMEIH, LIVE, AWG).

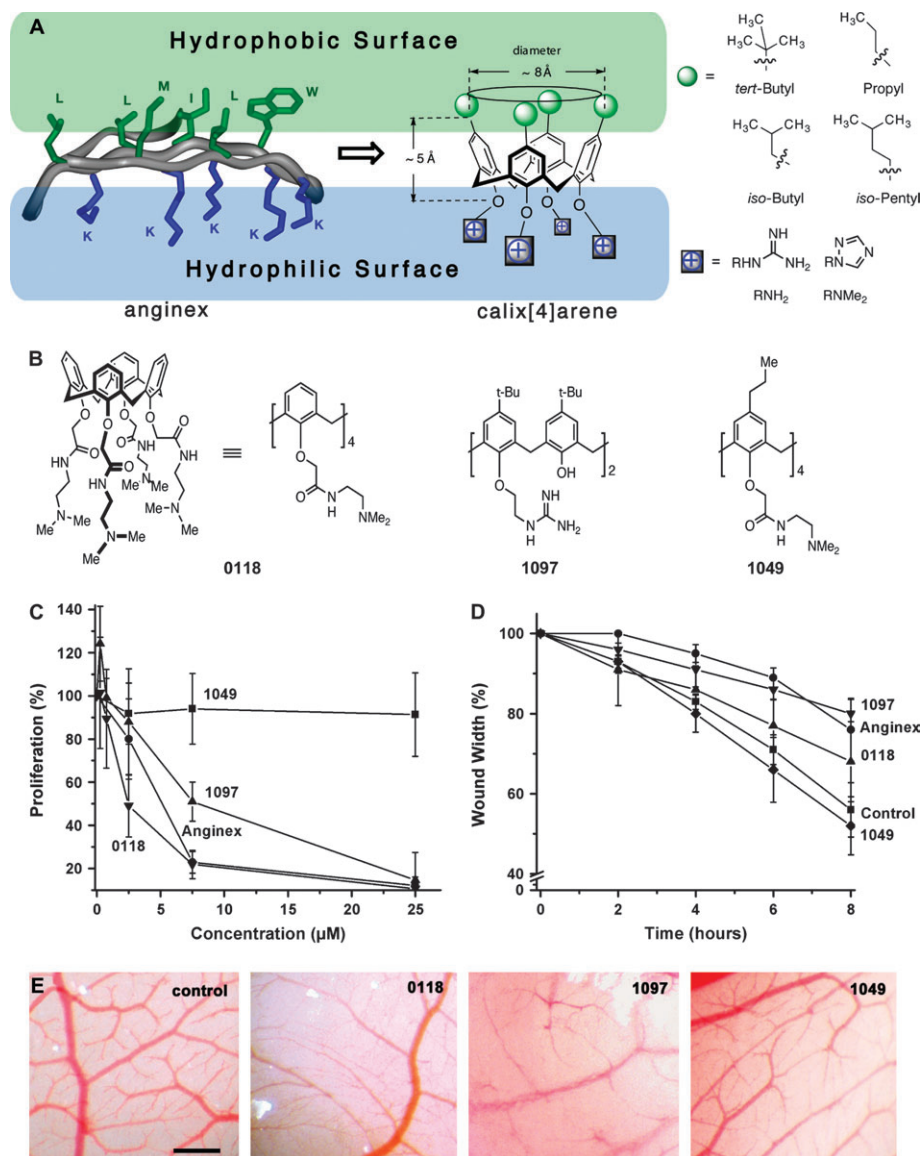
Correspondence to: Kevin H. Mayo, PhD, Department of Biochemistry, 6-155 Jackson Hall, University of Minnesota, 321 Church Street, Minneapolis, MN 55455 (e-mail: mayox001@umn.edu).

See “Notes” following “References.”

DOI: 10.1093/jnci/djj247

© The Author 2006. Published by Oxford University Press. All rights reserved. For Permissions, please e-mail: journals.permissions@oxfordjournals.org.

Fig. 1. Design of β -sheet topomimetics and in vitro activities. **A)** Topological design features influencing the choice of the calix[4]arene scaffold for arraying hydrophobic and hydrophilic substituents to mimic the structural and compositional characteristics of antiangiogenic proteins and peptides like anginex. **Left)** In the folded structure of anginex, hydrophobic and hydrophilic surfaces, as well as specific amino acid residues in one letter code, are indicated. **Middle)** The calix[4]arene scaffold is shown to scale. **Right)** The hydrophobic and basic group chemical substituents that were used on the two faces of the calix[4]arene scaffold. **B)** Two structural representations of the tetra-amine compound **0118** and two related analogs, diguanidine **1097** and tetraamine **1049**. t-Bu = tert-butyl; Me = methyl. **C)** Proliferation of basic fibroblast growth factor (bFGF)-stimulated human umbilical vein-derived endothelial cell (HUVEC) cultures treated with various doses of calixarene-derived compounds and anginex control relative to that observed without treatment (11). Results, initially calculated as mean counts per minute of three independent experiments each from triplicate cultures, are plotted as the percentage of proliferation relative to control, along with 95% confidence intervals (CI). **D)** Relative mean wound widths (\pm 95% CI) in HUVEC monolayers after treatment with calixarene derivatives or anginex. Data points represent the means obtained in three independent experiments, each using duplicate cultures. **E)** In vivo angiogenesis inhibition in the chorioallantoic membrane (CAM) assay caused by application of the calixarene analogs at a concentration of 25 μ M. Scale bar = 0.5 mm.



than anginex ($IC_{50} = 5 \mu\text{M}$, 95% CI = 4.0 μM to 5.9 μM) and **1097** slightly less potent ($IC_{50} = 8 \mu\text{M}$, 95% CI = 2.1 μM to 13.2 μM). Another analog, **1049**, had no effect on endothelial cell proliferation at the highest dose tested (25 μM) and was used further as a negative control.

We then measured the effect of the compounds on endothelial cell migration, another indicator of angiogenesis, using the wound healing assay (Fig. 1, D), as described previously (11). In brief, a wound was made in a confluent monolayer of HUVEC using a blunt glass pipette. The medium was replaced with medium containing 10 ng/mL bFGF, with or without 25 μM compound, and after 0, 2, 4, 6, and 8 hours, wound width was measured. In Fig. 1, D, wound widths in the presence of a given compound at particular time points are expressed in as a percentage of the initial

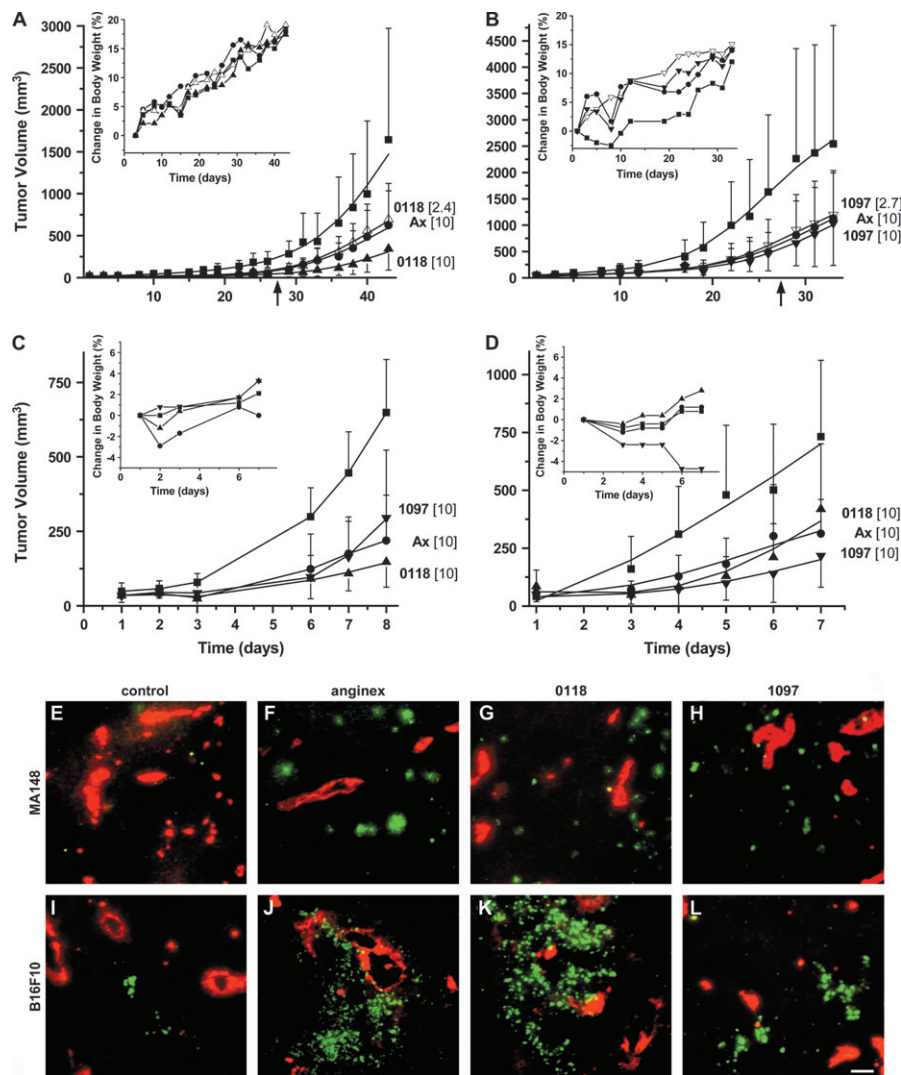
wound width (relative wound width). Wound healing (decrease in wound width) in **0118**-treated cultures was substantially reduced relative to that in control cultures with a wound width after 8 hours of 68% (95% CI = 58% to 78%) compared to 56% (95% CI = 49% to 63%) in untreated controls. Cultures treated with **1097** and anginex also showed a reduction in wound healing with relative wound widths after 8 hours of 80% (95% CI = 76% to 84%) and 76% (95% CI = 68% to 84%), respectively.

We also tested the angiostatic potential of these compounds using the chorioallantoic membrane (CAM) assay in fertilized chicken eggs (11) (Fig. 1, E). Angiostatic compounds (25 μM in 3% dimethyl sulfoxide [DMSO]-phosphate-buffered saline [PBS]) were applied daily to the membranes in aliquots of

65 μL from day 10 to day 13 after fertilization, and on day 14, the CAMs were photographed. Angiogenesis was reduced in the CAMs treated with **0118** and **1097**, but not with **1049**, compared with that in untreated controls. Although some vessels were still visible in **0118**- and **1097**-treated embryos, they appeared shorter, finer, and less defined than those in controls. Anginex had similar angiostatic effects in the CAM assay (12).

We next assessed the efficacy of **0118** and **1097** in two tumor growth models in mice [MA148 human ovarian and B16 mouse melanoma (11,13,14)] following protocols approved by the University of Minnesota Research Animal Resources Ethical Committee. Female athymic nude mice (nu/nu, 5–6 weeks old, $n = 7$ per group) or C57BL/6 male mice ($n = 10$ per group) purchased from the National Cancer Institute were inoculated

Fig. 2. Inhibition of tumor growth and angiogenesis in mice by calixarene derivatives in human ovarian and mouse melanoma models of tumorigenesis. (A–D) Tumor volumes (\pm 95% confidence intervals [CI], with only the upper or lower part of the CI line shown for clarity) in the human ovarian MA148 model (A and B) and the mouse melanoma B16F10 model (C and D) are plotted against days postinoculation. Curves were projected through mean values on growth curves by smooth spline fitting. In all panels, symbols are defined as \blacksquare = control, \bullet = anginex (Ax; 10 mg/kg), Δ = **0118** (2.4 mg/kg), \blacktriangle = **0118** (10 mg/kg), ∇ = **1097** (2.7 mg/kg), \blacktriangledown = **1097** (10 mg/kg). In panels A and B, an arrow indicates the end of treatment. As an indirect measurement of general toxicity, body weights of mice were monitored twice weekly (inserts to panels A–D). E–L) Reduced vessel density (red) and increased apoptosis (green) in mice treated with angiostatic compounds. MA148 tumor section staining (E–H) and B16F10 tumor section staining (I–L) are shown for vehicle-treated (E and I), anginex-treated (F and J), **0118**-treated (G and K), and **1097**-treated (H and L) mice. Images are representatives of the means for the amount of staining for a 10-mg/kg dose. Original magnification is 200 \times . Scale bar = 50 μ m. Digital images were stored and processed using Adobe Photoshop (Adobe Inc., Mountain View, CA).



in the right flank with 100 μ L of exponentially growing MA148 human ovarian carcinoma cells (2×10^7 cells/mL) or B16F10 murine melanoma cells (2×10^6 cells/mL), respectively, as described previously (11,13,14). Treatment with calixarene-based topomimetics or anginex was initiated when tumors reached volumes of 70 mm³ (MA148) or 80 mm³ (B16F10). All compounds were dissolved in PBS containing 15% v/v DMSO (control mice were treated with PBS containing an equivalent amount of DMSO) and were delivered subcutaneously using implanted osmotic minipumps (11,13,14). (For the experiments using the B16 model depicted in Fig. 2, D, compounds were administered by twice-daily intraperitoneal injection.) Anginex was administered at 10 mg/kg per day, a dose previously shown to inhibit tumor growth in the MA148 model by about 60% to 70% (11,13,14). Compounds **0118** (Fig. 2, A) and **1097**

(Fig. 2, B) were given at two doses: the pharmacologically equivalent dose of 10 mg/kg per day and the molar equivalent dose in the pumps of 2.4 mg/kg per day for **0118** and 2.7 mg/kg per day for **1097**. In the MA148 model, treatment was continued for 28 days and tumor growth was monitored for an additional 2 weeks after treatment. In the B16 model, treatment was given and tumor growth was monitored for 7 or 8 days. Tumor volumes were determined by measuring the dimensions of tumors using calipers and substituting the values into an equation for the volume of a spheroid: $(a^2 \times b \times \pi) / 6$, where a is the width and b the length of the tumor. At the conclusion of each experiment, tumors were excised from mice killed by cervical dislocation after being anesthetized (0.2 mL of 100 mg/kg ketamine and 10 mg/kg xylazine mixture, administered via intraperitoneal injection). Tumor weights correlated well with the calculated tumor volumes

(data not shown). Tumor growth was analyzed using a mixed-effects growth curve model by quadratic fitting of tumor growth curves against time (15), with treatment-specific coefficients for linear and quadratic terms of time, as well as within-subject random effects. To compare differences in tumor growth between any two treatment regimes, the log-likelihood ratio test was used (15), either with different or the same coefficients for linear and quadratic terms.

In the MA148 model (Fig. 2, A), ovarian tumor growth for the three treated groups as assessed at the end of the study (after treatment and additional monitoring) was reduced compared to that in control mice ($P < .001$): by 62% for anginex (95% CI = 23% to 100%), 58% for **0118** at 2.4 mg/kg (95% CI = 16% to 100%), and 79% for **0118** at 10 mg/kg (95% CI = 57% to 100%). Using **1097** in the MA148 model (Fig. 2, B), tumor growth in mice was also reduced relative

to that in control-treated mice. At the end of the study, **1097** inhibited MA148 tumor growth on average by 53% at 2.4 mg/kg (95% CI = 2% to 100%) or 59% at 10 mg/kg (95% CI = 12% to 100%). After cessation of treatments, the rate of tumor growth began to increase, but even 2 weeks later, tumor growth inhibition remained pronounced (Fig. 2, A and B).

Against the more aggressive B16 melanoma, a syngeneic model in immunocompetent mice (11), tumor growth curves for all treated groups were also different from those of tumors in control mice ($P < .001$), whether administration was by osmotic minipumps implanted subcutaneously (Fig. 2, C) or by twice-daily intraperitoneal injection (Fig. 2, D). At the end of the study, **0118** had inhibited growth on average by 77% (95% CI = 63% to 92%) relative to control treatment when administered via minipumps and 42% (95% CI = 0% to 88%) when administered by injection, whereas **1097** inhibited growth by 54% (95% CI = 18% to 91%) and 70% (95% CI = 48% to 93%), respectively. In comparison, anginex inhibited tumor growth by 66% (95% CI = 41% to 91%) when administered subcutaneously by osmotic minipump and 57% (95% CI = 30% to 85%) when administered intraperitoneally.

Treatment with **0118**, **1097**, or anginex did not cause observable toxicity, as assessed by behavior, body weight change, or hematocrit or creatinine levels (both determined by blood drawing on the last day of treatment). Overall, body weights increased irrespective of treatment, with the exception of a slight decrease in body weights in B16 mice injected with **1097** (inserts to Fig. 2, A–D). Upon autopsy, we observed no readily apparent abnormalities in internal organs.

Microvessel density in sections of tumors removed at the end of the experiment was analyzed histochemically (Fig. 2, E–L) using a phycoerythrin-labeled anti-CD31 antibody (PECAM-1; Pharmingen, San Diego, CA) and quantified as described previously (16). Tumors of mice treated with anginex (Fig. 2, F and J), **0118** (Fig. 2, G and K), and **1097** (Fig. 2, H and L) showed marked and statistically significant decreases in microvessel density relative to tumors in control mice (Fig. 2, E and I), as quantified in Supplemental Table 1 (available at <http://jncicancerspectrum.oxfordjournals.org/jnci/content/vol98/issue13>).

oxfordjournals.org/jnci/content/vol98/issue13). These compounds also had statistically significant effects on vessel architecture, as evidenced by declines in the number of vessels, vessel branch points, and vessel length relative to control (Supplemental Table 2, available at <http://jncicancerspectrum.oxfordjournals.org/jnci/content/vol98/issue13>).

We also investigated whether treatment with the compounds increased the rate of apoptosis of tumor cells by subjecting tumor sections to the terminal deoxynucleotidyl transferase-mediated dUTP-nick-end fluorescein labeling assay for DNA fragmentation according to the manufacturer's instructions (In Situ Cell Death Detection Kit, Fluorescein; Roche, Indianapolis, IN). After a 1-hour incubation with the enzyme at room temperature, slides were washed with PBS and immediately imaged using an Olympus BX-60 fluorescence microscope at 200 \times magnification, as previously described (16). Apoptosis was quantified as described earlier (16), and values have been provided in Supplemental Table 1 (available at <http://jncicancerspectrum.oxfordjournals.org/jnci/content/vol98/issue13>).

Although the concept of designing protein surface mimetics has existed for many years (17), the approach usually was based on constrained or cyclized peptides derived from a larger protein, as exemplified by mimetics of α -helices (18–20), β -strands (21), β -sheets (22,23), β -turns (24–26), and loops (27–29). There are only a few examples of designed nonpeptidic topomimetic compounds that mimic a surface of a protein or peptide; one uses an oligosaccharide (30) and the other uses a linear aromatic template (19) to arrange chemical substituents with similar distances and orientations like those found in helical peptides. Here, we have reported the use of the calix[4]arene scaffold to design compounds that mimic the surface topology of β -sheet peptides. Even though these compounds do indeed have similar overall molecular dimensions as a segment of β -sheet-folded anginex and, like anginex, are amphipathic, they do not exactly match its surface topology, leaving the question open as to whether they are true mimetics of anginex. In fact, because the positively charged, amphipathic β -sheet structural motif is common to most antiangiogenic proteins and peptides (6), **0118** or **1097** could be mimetics of any of them or target some

as yet unidentified receptor. Nevertheless, we have apparently captured elements of biological import in these two topomimetics (**0118** and **1097**), both of which are antiangiogenic and antitumor agents suitable for further pre-clinical analysis.

Although anginex and some other angiogenesis inhibitors including endostatin, angiostatin, and Avastin are proteins, nonpeptidic compounds generally make for superior pharmaceutical drugs, primarily because they often exhibit greater in vivo exposure, can be administered orally, lack an immune response, and/or are less expensive to produce. It is for these reasons that protein surface topomimetics **0118** and **1097** may stand as the new generation of antiangiogenic agents for use in the clinic against cancer. The next steps are to assess how these agents behave pharmacokinetically and pharmacodynamically and to prepare a complete toxicology profile in animals, prior to initiating a phase I clinical trial in humans.

REFERENCES

- (1) Griffioen AW, Molema G. Angiogenesis: potentials for pharmacologic intervention in the treatment of cancer, cardiovascular diseases, and chronic inflammation. *Pharmacol Rev* 2000;52:237–68.
- (2) O'Reilly MS, Boehm T, Shing Y, Fukai N, Vasios G, Lane WS, et al. Endostatin: an endogenous inhibitor of angiogenesis and tumor growth. *Cell* 1997;88:277–85.
- (3) Boehm T, Folkman J, Browder T, O'Reilly MS. Antiangiogenic therapy of experimental cancer does not induce acquired drug resistance. *Nature* 1997;390:404–7.
- (4) Ferrara N, Hillan KJ, Gerber HP, Novotny W. Discovery and development of bevacizumab, an anti-VEGF antibody for treating cancer. *Nat Rev Drug Discov* 2004;3:391–400.
- (5) Chen H, Herndon ME, Lawler J. The cell biology of thrombospondin-1. *Matrix Biol* 2000;19:597–614.
- (6) Dings RP, Nesmelova I, Griffioen AW, Mayo KH. Discovery and development of antiangiogenic peptides: a structural link. *Angiogenesis* 2003;6:83–91.
- (7) Dings RP, Arroyo MM, Lockwood NA, Van Eijk LI, Haseman JR, Griffioen AW, et al. Beta-sheet is the bioactive conformation of the anti-angiogenic anginex peptide. *Biochem J* 2003;23:281–8.
- (8) Mayo KH, Dings RP, Flader C, Nesmelova I, Hargittai B, van der Schaft DW, et al. Design of a partial peptide mimetic of anginex with antiangiogenic and anticancer activity. *J Biol Chem* 2003;278:45746–52.
- (9) Gutsche CD, Bauer LJ. Calixarenes. 13. The conformational properties of calix[4]arenes,

- calix[6]arenes, calix[8]arenes, and oxacalixarenes. *J Am Chem Soc* 1985;107:6052–9.
- (10) Gutsche CD, Dhawan B, Levine JA, No KH, Bauer LJ. Calixarenes. 9. Conformational isomers of the ethers and esters of calix[4]arenes. *Tetrahedron* 1983;39:406–26.
- (11) van der Schaft DW, Dings RP, de Lussanet QG, van Eijk LI, Nap AW, Beets-Tan RG, et al. The designer anti-angiogenic peptide anginex targets tumor endothelial cells and inhibits tumor growth in animal models. *FASEB J* 2002;16:1991–3.
- (12) Griffioen AW, van der Schaft DW, Barendsz-Janson AF, Cox A, Struijker Boudier HA, Hillen HF, et al. Anginex, a designed peptide that inhibits angiogenesis. *Biochem J* 2001;354:233–42.
- (13) Dings RP, Yokoyama Y, Ramakrishnan S, Griffioen AW, Mayo KH. The designed angiostatic peptide anginex synergistically improves chemotherapy and antiangiogenesis therapy with angiostatin. *Cancer Res* 2003;63:382–5.
- (14) Dings RP, van der Schaft DW, Hargittai B, Haseman J, Griffioen AW, Mayo KH. Antitumor activity of the novel angiogenesis inhibitor anginex. *Cancer Lett* 2003;194:55–66.
- (15) Pinheiro JC, Bates DM. Mixed-effects models in S and S-plus. 1st ed. New York (NY): Springer-Verlag; 2000. p. 528
- (16) Wild R, Ramakrishnan S, Sedgewick J, Griffioen AW. Quantitative assessment of angiogenesis and tumor vessel architecture by computer-assisted digital image analysis: effects of VEGF-toxin conjugate on tumor microvessel density. *Microvasc Res* 2000;59:368–76.
- (17) Fairlie DP, West ML, Wong AK. Towards protein surface mimetics. *Curr Med Chem* 1998;5:29–62.
- (18) Yin H, Hamilton AD. Terephthalamide derivatives as mimetics of the helical region of Bak peptide target Bcl-xL protein. *Bioorg Med Chem Lett* 2004;14:1375–9.
- (19) Yin H, Lee GI, Sedey KA, Rodriguez JM, Wang HG, Sebti SM, et al. Terephthalamide derivatives as mimetics of helical peptides: disruption of the Bcl-x(L)/Bak interaction. *J Am Chem Soc* 2005;127:5463–8.
- (20) Kelso MJ, Beyer RL, Hoang HN, Lakdawala AS, Snyder JP, Oliver WV, et al. Alpha-turn mimetics: short peptide alpha-helices composed of cyclic metallopentapeptide modules. *J Am Chem Soc* 2004;126:4828–42.
- (21) Loughlin WA, Tyndall JD, Glenn MP, Fairlie DP. Beta-strand mimetics. *Chem Rev* 2004;104:6085–117.
- (22) Schneider JP, Kelly JW. Templates that induce alpha-helical, beta-sheet, and loop conformations. *Chem Rev* 1995;95:2169–87.
- (23) Nowick JS, Pairish M, Lee IQ, Holmes DL, Ziller JW. An extended beta-strand mimic for a larger artificial beta-sheet. *J Am Chem Soc* 1997;119:5413–24.
- (24) Eguchi M, Kahn M. Design, synthesis, and application of peptide secondary structure mimetics. *Mini Rev Med Chem* 2002;2:447–62.
- (25) Kee KS, Jois SD. Design of beta-turn based therapeutic agents. *Curr Pharm Des* 2003;9:1209–24.
- (26) Perkins JJ, Duong LT, Fernandez-Metzler C, Hartman GD, Kimmel DB, Leu CT, et al. Non-peptide alpha(v)beta(3) antagonists: identification of potent, chain-shortened RGD mimetics that incorporate a central pyrrolidinone constraint. *Bioorg Med Chem Lett* 2003;13:4285–8.
- (27) Sheppard GS, Kawai M, Craig RA, Davidson DJ, Majest SM, Bell RL, et al. Lysyl 4-aminobenzoic acid derivatives as potent small molecule mimetics of plasminogen kringle 5. *Bioorg Med Chem Lett* 2004;14:965–6.
- (28) Hasegawa A, Cheng X, Kajino K, Berezov A, Murata K, Nakayama T, et al. Fas-disabling small exocyclic peptide mimetics limit apoptosis by an unexpected mechanism. *Proc Natl Acad Sci U S A* 2004;101:6599–604.
- (29) Alexopoulos K, Fatseas P, Melissari E, Vlahakos D, Roumelioti P, Mavromoustakos T, et al. Design and synthesis of novel biologically active thrombin receptor non-peptide mimetics based on the pharmacophoric cluster Phe/Arg/NH₂ of the Ser42-Phe-Leu-Leu-Arg46 motif sequence: platelet aggregation and relaxant activities. *J Med Chem* 2004;47:3338–52.
- (30) Xuereb H, Maletic M, Pelczer I, Gildersleeve J, Kahne D. Design of an oligosaccharide scaffold that binds in the minor groove of DNA. *J Am Chem Soc* 2000;122:1883–90.

NOTES

Supported by a research grant from the National Cancer Institute (R01 CA-096090 to K. H. Mayo).

K. H. Mayo has a financial interest in a company that has licensed compounds discussed in this paper from the University of Minnesota.

R. P. M. Dings and X. Chen contributed equally to this work.

Manuscript received September 15, 2005; revised April 27, 2006; accepted May 15, 2006.